PACS NUMBER: 61.05.CM, 61.46.HK, 62.20.QP.68.37.HK, 81.15.-Z

STRUCTURE, PROPERTIES AND MORPHOLOGY OF NANOSTRUCTURED COATINGS SOLID Ti-Si-N

M.V. Kaverin[1], B. Zhollybekov[2]
[1]*Sumy State University*
Ukraine
[2]*Karakalpak State University (Nukus)*
Uzbekistan
Received 12.08.2013

The work presents a comparative analysis of results obtained from samples of nanostructured Ti-Si-N coatings. Element composition, defect structure, concentration of elements throughout the depth of coating and morphology of films were studied using the techniques of slow positron beam (SPB), X-ray photoelectron spectroscopy (XPS), Rutherford backscattering spectrometry (RBS), proton microbeam (μ-PIXE), X-ray diffraction (XRD), scanning electron microscopy with energy – dispersive analysis (SEM with EDS). Results of mentioned above experiments showed that changing the substrate potential during deposition of coatings the stoichiometry and morphology of obtained coatings changes too. After thermal treatment up to 600 °C the formation of two phases: solid solution of TiN, and amorphous or quasi-amorphous α-SiN_x (Si_3N_4) envelope was observed. During experiments the grain size did not change significantly, while the extra energy was used for the completion of the spinodal (phase) segregation.

СТРУКТУРА, СВОЙСТВА И МОРФОЛОГИЯ ТВЕРДЫХ НАНОСТРУКТУРИРОВАННЫХ ПОКРЫТИЙ Ti-Si-N
М.В. Каверин, Б. Жоллыбеков

В работе представлен сравнительный анализ результатов, полученных на образцах наноструктурированных покрытий Ti-Si-N. Элементный состав, дефектная структура, концентрация элементов по глубине покрытия и морфология пленок были изучены с использованием таких методов как пучок медленных позитронов (SPB), рентгеновской фотоэлектронной спектроскопии (РФЭС), резерфордовского обратного рассеяния (RBS), протонного микропучка (μ-PIXE), рентгеноструктурного анализа (РСА), сканирующей электронной микроскопии с энергодисперсионным анализом (SEM с EDS). Результаты указанных выше экспериментов показали, что изменение потенциала подложки во время нанесения покрытий приводит к изменению стехиометрии и морфологии получаемых покрытий. Кроме того после термической обработки до 600 °С наблюдается образование двух фаз: твердого раствора TiN и аморфной или квазиаморфной фазы α-SiN_x(Si_3N_4). В ходе экспериментов размер зерна не изменился, а дополнительная термическая обработка способствовала завершению спинодальный (фазовой) сегрегации.

СТРУКТУРА, ВЛАСТИВОСТІ ТА МОРФОЛОГІЯ ТВЕРДИХ НАНОСТРУКТУРОВАНИХ ПОКРИТТІВ Ti-Si-N
М.В. Каверін, Б. Жоллибеков

У роботі представлений порівняльний аналіз результатів, отриманих на зразках наноструктурованих покриттів Ti-Si-N. Елементний склад, дефектна структура, концентрація елементів за глибиноюпокриття та морфологія плівок були досліджені з використанням таких методів як пучок повільних позитронів (SPB), рентгенівської фотоелектронної спектроскопії (РФЕС), резерфордівського зворотнього розсіювання (RBS), протонного мікропучка (μ-PIXE), рентгеноструктурного аналізу (РСА), скануючої електронної мікроскопії з енергодисперсійним аналізом (SEM з EDS). Результати зазначених вище експериментів показали, що змінювання потенціалу підкладки під час нанесення покриттів призводить до змінювання стехіометрії та морфології одержаних покриттів. Крім того після термічної обробки при 600 °С спостерігається утворення двох фаз: твердого розчину TiN та аморфної або квазіаморфної фази α-SiN_x(Si_3N_4). У ході експериментів розмір зерна не змінився, а додаткова термічна обробка сприяла завершенню спінодальної (фазової) сегрегації.

INTRODUCTION

One of the most important problems of modern materials science is fabrication and construction of new materials with unique functional properties [1–8]. Nanostructure materials with high hardness, elasticity modulus, thermal stability, wear and corrosion

resistance belongs to such materials [9 – 11]. There is a large variety of different coating's systems, but Ti-Si-N coatings stand separately due to its unique properties and characteristics. That is why it is very important to study such nanostructure coatings and to obtain new information about structure of defects, phase composition, physical and mechanical properties, and this task seems to be an actual problem of modern physics of solids.

It is well known from literature [3, 5], that adding of Si to the TiN coating leads to increasing of the coating's hardness and temperature resistance. At a specified concentration of Si, which equals to (5 ÷ 12)% it also leads to forming of two-phases composite with TiN and α-SiNx phases.

EXPERIMENT DETAILS

We used a Cathodic-Arc-Vapor-Deposition device "Bulat –3T" with HF generator [3, 5]. Potential bias was applied to the substrate from HF generator of pulsed damped oscillations, it frequency was less than 1 MHz. The duration of each pulse was 60 μs; repetition rate was about 10 kHz. The amount of negative self-bias potential of the substrate caused by HF diode effect was 2 ÷ 3 kV. Using steel 3 samples (2 mm thickness, 20 mm diameter, polished surface), we deposited coatings on the device with cathodic vacuum-arc vaporizer in high-frequency discharge (two cathodes, made of Ti and Si). Atomic Nitrogen was injected into the chamber. Thickness of the obtained coating was near 2.2 μm.

For TiN coatings fabrication we used Ti of the grade BT-1-00. Thickness of all coatings was 2.2 μm. Deposition parameters are presented in the tabl. 1.

Table 1

Physical and technical parameters of deposition of coatings

Deposited material	Coating	I, A	P_N, Pa	U_{hv}, V	U_b, B	Remarks
Ti	TiN	90	0.3	200	200	Pulse high-frequency technology
Ti + Si	Ti-Si-N	100	0.3	200	–	Pulse high-frequency technology
Ti + Si	Ti-Si-N	100	0.7	200	–	Pulse high-frequency technology

Phase composition and structure researching were provided on the X-ray diffractometer DRON-3M in CuKα irradiation using graphite monochromator in secondary beam. Diffraction spectrums were obtained in pointwise regime with a scanning step 2 = 0.05 … 0.10. For stress analysis, we used X-ray tensometry ("α-sin^{2}ψ"-method) and its modifications, which are valid for coatings with strong axial type texture [12, 13].

Elementary composition of the coatings was studied using Rutherford backscattering of $^4He^+$ ions with 1.7 MeV energy, detector resolution $E = 13$ keV, dispersion angle ≈1700. Also we used scanning electron microscopy (SEM) with energy dispersion analysis (Jeol 7000F microscope, Japan) in contrast of electrons and in direct and backscattering electron reflection. For surface morphology investigations, we used atomic-force microscopy AFM Objective to obtain 3D image of surface topography, electron-ion scanning microscope Quanta 200 3D with roentgen-fluorescent microanalyzer EDAX with appropriate software, and automatic contact precision profilometer SURTRONIC 25.

Nanohardness and elastic modulus measurements were done using trihedral Berkovich indentor (Nano Indenter G200, TN, USA, Oak Ridge, Nano Instruments Innovation Center). For analysis of vacancy-type defects in the coating we used slow positron beam (Halle, Germany). We measured S-parameter of the Doppler broadening annihilation peak (DBAP) by changing energy of the fallen positron beam from 1 KeV to 30 KeV, and that allowed us to change the analysis depth [14,15].

The bonding states were determined using photoelectron spectroscopy (XPS, Kratos AXIS Ultra) with a monochromatic AlK (1486.71 eV, X-ray radiation 15 kV/10 mA).

EXPERIMENTAL RESULTS AND DISCUSSION

Fragments of diffraction spectrums for Ti-Si-N samples (as deposited and after annealing under the temperature 600 °C for 30 min) are presented on fig. 1. We calculated lattice parameter $a_0 = 0.42462$ A and found strong texture (111) (Ti, Si) N and (222) (Ti, Si) N (see curves 1 and 2).

In addition, we detected small peaks from TiO_2 (JCPDS-19-370). Volume fraction of oxides after thermal annealing in the chamber is low and it is not higher than 5%.

Stresses analysis showed, that there is high compression deformation in (Ti, Si)N hard solution

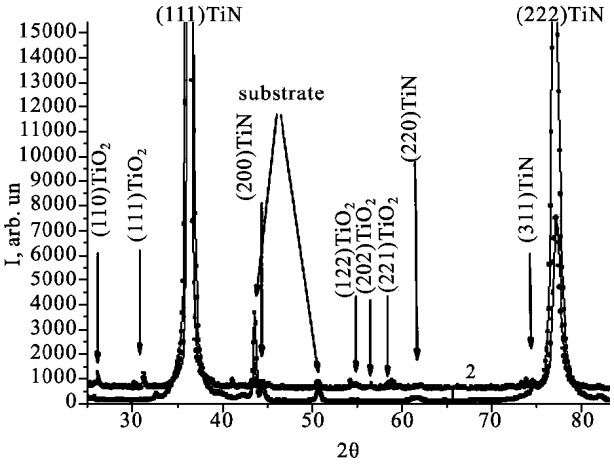

Fig. 1. Ti-Si-N coating's X-ray diffraction patterns: 1) as deposited; 2) after annealing under the temperature 600 °C for 30 min, vacuum $P = 50$ mbar.

(equals to – 2.6%) and it is reduced to the value of – 2.3% after annealing.

Coherent-scattering region evaluation (using Sherrer methodic) showed that size of nanograins increased from 12.5 nm to 13 nm, and when initial size of nanograins is 25 nm, it increased to (28 ÷ 30) nm. In other words, due to annealing under the temperature of 600 °C for 30 minutes, insignificant changing of grain size is observed, and rest part of energy was used on finishing of spinodal segregation process, forming of monolayer α-Si_3N_4.

We can make an interim conclusion, that when compression deformation and order of structuring are high, annealing under the temperature of 600 °C for 30 minutes do not lead to catastrophic changes both in phase composition, structure and mode of deformation. Layer, made of (Ti, Si)N solid solution, is formed, and silicon-nitrogen phase is also formed around nanograins. In according to it, Si concentration is reduced in solid solution; some amount of Ti atoms creates TiO_2 film on the coating's surface. Ti-Si-N coatings structure is characterized by high level of microdeformations of lattice (more than 1%) [9]. High value of microdeformations of lattice probably indicates on inhomogeneity of chemical structure in every phase of the coating. Coatings have strong texture [6]. Condensation compressive stresses leads to (111) texture forming in (Ti, Si)N solid solution films. Using approximation methods we defined average crystallites sizes of the (Ti, Si)N solid solution, and it varies from 12.5 to 25 nm. The obtained coatings have next hardness: TiN ($H = 28$ GPa, $E = 312$ GPa); Ti-Si-N ($H = 38 \div 39$ GPa, $E = 356$ GPa).

In tabl. 2, we summarized results of tribological investigations. It is clearly seen from this results, that

Table 2

Tribological properties of nanocomposite coatings

Coating	Temperature, °C	Wear factor, coating, mm^3/nm	Wear counter body mm^3/nm	Friction coefficient
Ti-Si-N	30	$7.69 \cdot 10^{-5}$	$3.28 \cdot 10^{-5}$	0.88
	300	$2.63 \cdot 10^{-5}$	$3.49 \cdot 10^{-5}$	0.82
	600	$1.95 \cdot 10^{-5}$	$2.75 \cdot 10^{-5}$	0.69
TiN	30	$6.75 \cdot 10^{-5}$	$3.30 \cdot 10^{-5}$	0.81
	300	$3.62 \cdot 10^{-5}$	$3.51 \cdot 10^{-5}$	0.87
	600	$5.16 \cdot 10^{-5}$	$3.83 \cdot 10^{-5}$	0.91

wear coefficient for TiN coating increases with temperature increasing, but for Ti-Si-N coating wear coefficient decreases to 0.69 ($T = 500$ °C), which is approximately on 25% less, than under room temperature.

Elementary analysis results are presented on fig. 2, it was obtained using RBS method and EDS (energy-dispersion spectroscopy). As it is clearly seen from fig. 2a), Si concentration is less than 5 at.%, N concentration ≈ (35 ÷ 40) at.%, rest one is Ti, and for fig. 2b) N concentration ≈ 50 at.%, Ti ≈ 44 at.%, Si ≈ 5.5 at.%. Coating's thickness equals to 2.18 ± 0.01 μm in according to RBS data.

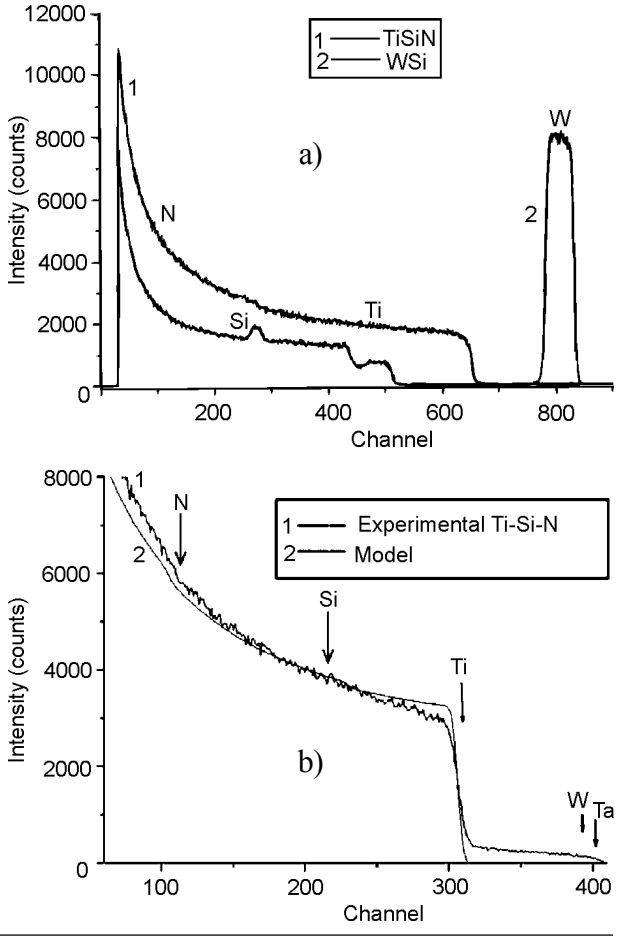

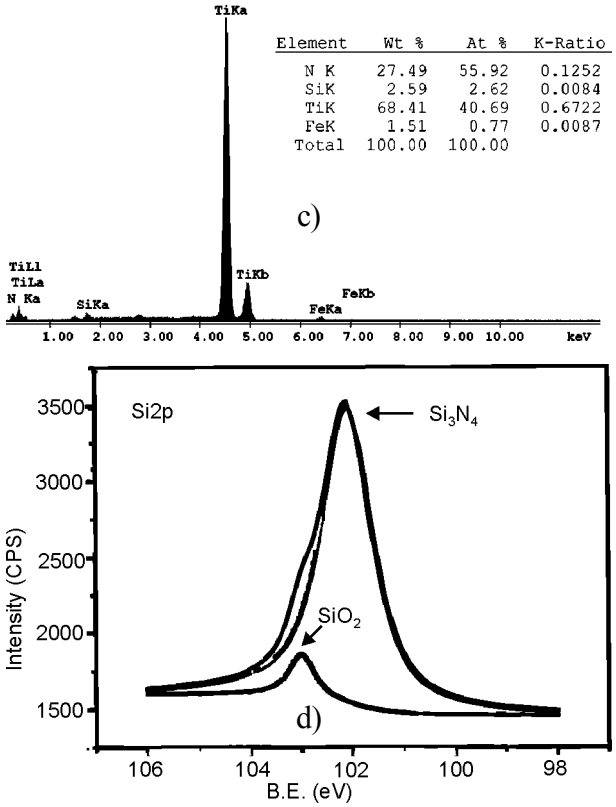

Fig. 2. Energy spectrums for samples with Ti-Si-N coatings; (a) bias potential –50 V, *PN* = 0.5 Pa (RBS), second curve corresponds to etalon SiW curve (for comparing); (b) bias potential –100 V, *PN* = 0.7 Pa (RBS); (c) bias potential –50 V, *PN* = 0.5 Pa (EDX); (d) XPS spectra obtained from Ti-Si-N coating.

RBS data confirms by EDX results, see fig. 2c). Concentration of Si in the coating is 2.62 at.%, Ti ≈40.69 at.%, N ≈ 55.92 at.%. For another series of samples (with Si concentration ≥ 5.8 at.%) we provided investigations of Si-Nx connection using XPS analysis. It showed high peak on 101.9 eV, and it points directly on forming of Si-Nx connection in this sample. But also we had a small peak, which points on forming of a very few amount of Si-O on 103.9 eV (after annealing in the air under the temperature of 600 °C for 30 min). Additional μ-PIXE investigations showed SiN forming on TiN nanograins borders.

Images of the coating's surface before and after annealing, under the temperature 600 °C (for 30 min.) are presented on fig. 3. We can observe flat "drops" of melted phase, no matter of HF stimulation. We should note that part of plasma jet consists of drop fractions, and we did not make analysis of such fractions.

To obtain a real thickness of Ti-Si-N nanostructure coating and to norm the depth of slow positron beam analysis, we cut a circle hole, through the coating thickness. As it is seen from fig. 3c), coating's thickness equals to 2.39 ÷ 2.41 μm. Calculation of positrons penetration depth shows that E_{max} = 20 keV, it corresponds to 2.11 μm of thickness. Even if we will take into account diffusion of thermalized positrons (it length is $L \approx 100$ nm), we will see that positron beam cannot reach interface between coating and substrate. That is why profiles of mean positron's penetration depths give us information about vacancy-type defects on the whole thickness of Ti-Si-N coating, but the interface border is not really achieved by them.

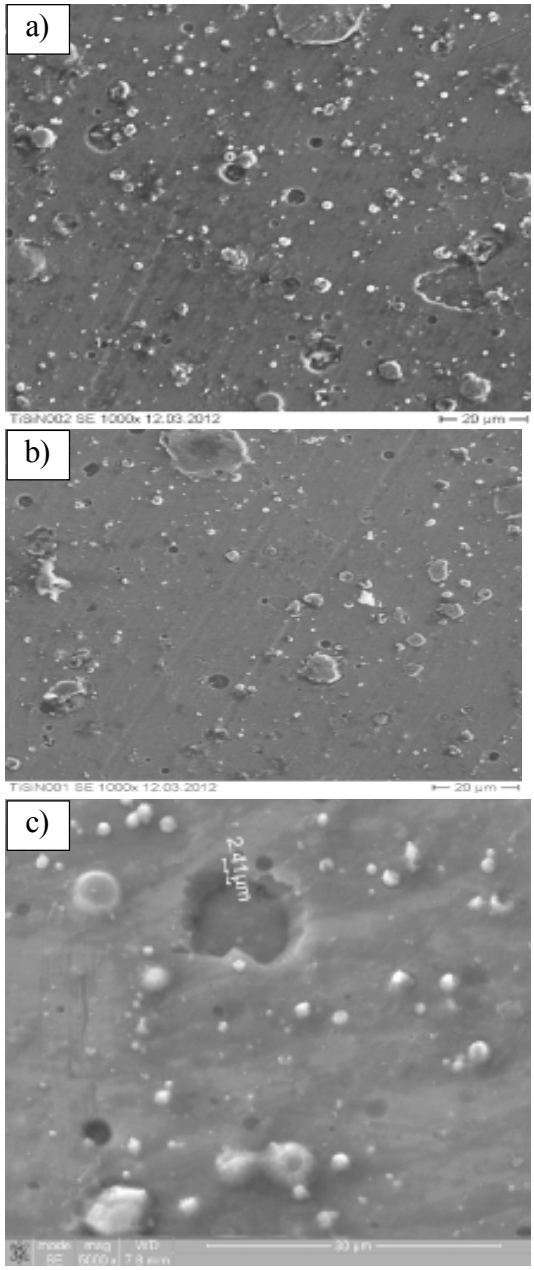

Fig. 3. Surface topography of the Ti-Si-N coating; (a) as deposited state; (b) after annealing under the temperature of 600 °C; (c) SEM-analysis of circle cross-section, which was obtained using ion beam cutting.

Positron annihilation method is the most effective, responsive and reliable method of analysis of free volumes in nanocrystalline materials (it has possible interval of defect's analysis in the range $10^{-6} \pm 10^{-3}$ defects per atom) [14, 15]. Part of positrons can be captured on the interface of two neighboring nanograins or on boundary junction of three neighboring nanocrystals. It gives us good opportunity to solve one of the most complicated and interesting problems of nanomaterials to understand structure (including electron structure) of the interfaces between nanograins, because length (volume) of such interfaces influences a lot on properties of nanocomposite coatings [1 – 9].

Fig. 4 shows dependence of S-parameter on energy, in other words, we can see profiles of defects in Ti-Si-N coating before (black curve) and after (red curve) thermal annealing under the temperature of 600 °C (30 min).

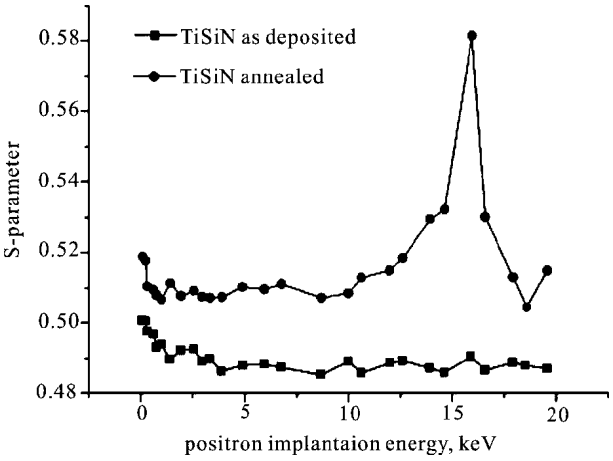

Fig. 4. Dependence of S-parameter on energy of positron microbeam (black curve as deposited coating, red curve annealed coating).

Significant changes in electron and defect structure of the coating is clearly seen from this figure. We should note, that defects concentration increases on the whole thickness of the coating, all positrons locates and annihilates on defects, which are situated on the boundaries of nanograins. Depth of diffusion of thermalized positrons is ≈100 nm, size of nanograins is (12.5 ÷ 13) nm, so we can say that almost all positrons are captured on interface's defects. As approaching to the interface between coating and substrate, *S*-parameter significantly increases, i.e. defects also migrate to the interface between coating and substrate due to thermal diffusion. Thickness of this transition layer of defects is no more than 250 nm. Calculation of vacancy defects concentration was done using positron capture model with two types of vacancy defects [12], and it showed that defects concentration increases after annealing from $5 \cdot 10^{16}$ to $7.5 \cdot 10^{17}$ cm^{-3}, thermally activated vacancies concentration also increases from $1 \cdot 10^{16}$ to $5 \cdot 10^{18}$ cm^{-3} (see red curve).

Loading and unloading curves are presented on fig. 5.

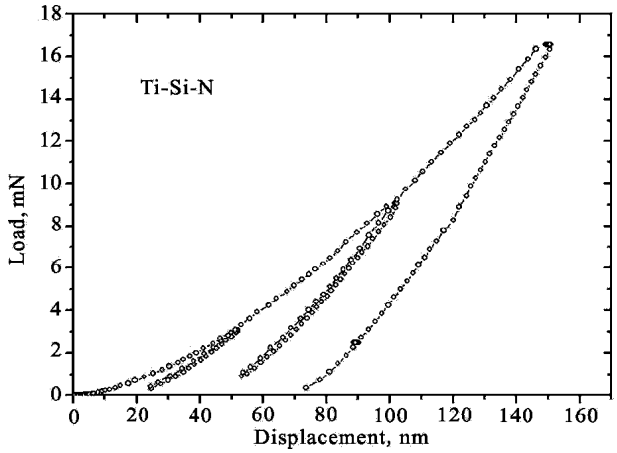

Fig. 5. Loading and unloading curves, obtained for Ti-Si-N coating ($U = -100$ V, $Pn = 0.7$ Pa), indentation on 50, 100 and 150 nm depth.

Nanoindentor penetrates on the surface layer of the Ti-Si-N coating (three different loadings). As it is seen from calculations, based on Oliver-Pharr methodic, an average hardness for such deposition regimes is 38.7 GPa, elasticity modulus is 370 ± 12 GPa. Annealing under the temperature of 600 °C in vacuum leads to increasing of elasticity modulus to values (430 – 448) GPa, it is connected with finishing of process of spinodal segregation on the boundaries of nanograins, i.e. with forming of thin SiN (Si_3N_4) interlayer (amorphous and quasi amorphous phases).

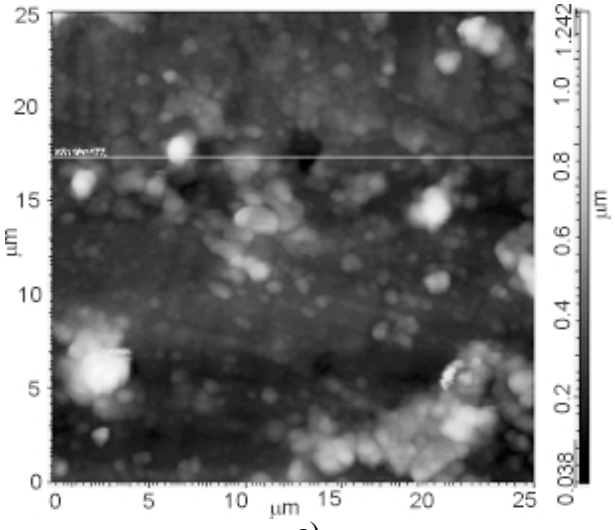

a)

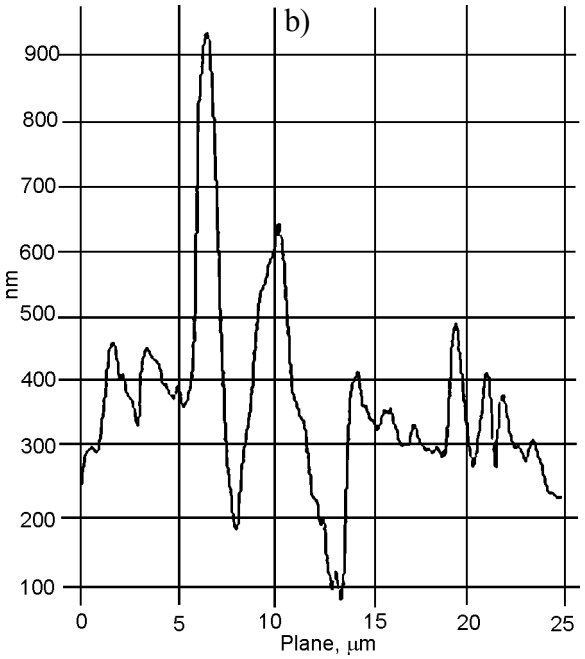

Fig. 6. An image of the surface topography of Ti-Si-N coating: a) – the surface area of 25×25 мм; b) – profilogram of Ti-Si-N coating from 100 to 900 nm roughness.

Fig. 6 shows a surface topography of Ti-Si-N nanostructured coatings. On the surface region of 25×25 μm can be seen a variation in depths.

Moreover, thermal annealing under the temperature of 600 °C in vacuum also changes Ti-Si-N coating's surface morphology (fig. 7).

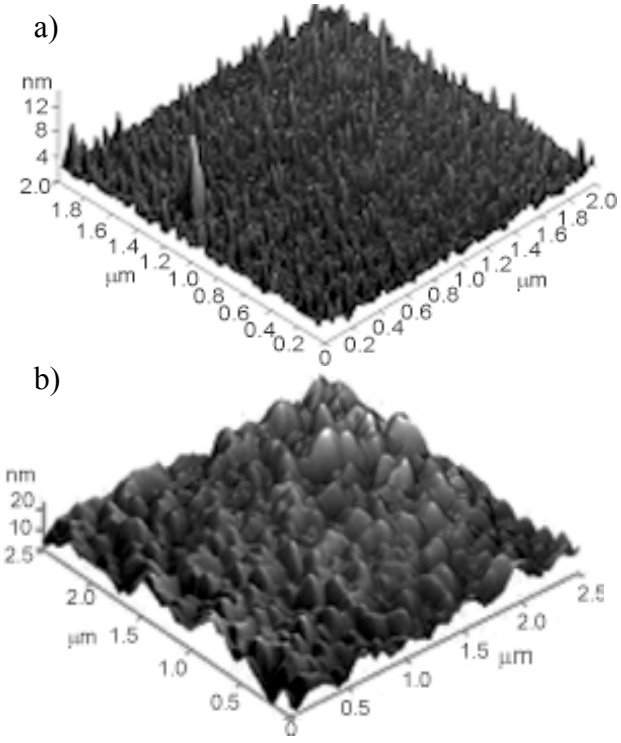

Fig. 7. Ti-Si-N coating's surface morphology: (a) 3d AFM image; (b) after annealing under the temperature of 600 °C.

We observed decreasing of an average roughness size, increasing of amount of defects (it is obvious from fig. 6).

After analysis we can say, that structure of defects changes on nanograins interfaces due to annealing, average roughness size decreases, nanohardness increases on 20% (in comparison with as deposited state) and it correlates with our previous works [13, 16]. Friction ratio decreases on 25% it is the main difference as opposed to works [17 – 19].

ACKNOWLEDGEMENTS

Authors thanks A.D. Pogrebnjak (Sumy, Ukraine) for measuring of profiles defects using slow positron beam, G. Abrasonis (Dresden, Germany) for elements' composition studies using RBS-analysis, V.M. Beresnev (Kharkov, Ukraine), D.A. Kolesnikov (Belgorod, Russia) and R. Krause-Rehberg (Halle, Germany). The work was done under financial support of Ministry of Education and Science of Ukraine (state program, order No. 411), and in collaboration with NIMS (Tsukuba, Japan) and Martin-Luther University (Dresden, Germany). The work was supported by Ministry of Education and Science of Ukraine (project No. 011U001382). Authors are grateful to the staff of the Joint Research Center "Diagnostics of Structure and Properties of Nanomaterials" (Belgorod State University, Russia) for their assistance with instrumental analysis.

REFERENCES

1. Gleiter H. Nanocrystalline materials//Progress in Materials Science. – 989.– Vol. 33.– P. 233-315.
2. Siegel R.W. Cluster-Assembled Nanophase Materials//Annual Review of Materials Science. – 1991. – Vol. 21. – P. 559-579.
3. Veprek S., Reiprich S.A. Concept for the design of novel superhard coatings//Thin Solid Films. – 1995. – Vol. 268. – P. 64-71.
4. Pogrebnyak A.D., Shpak A.P., Azarenkov N.A., Beresnev V.M. Structures and properties of hard and superhard nanocomposite coatings//Physics-Uspekhi. –2009. – Vol. 52. – P. 29-54.
5. Mayrhofer P.H., Mitterer C., Hultman L., Clemens H. Microstructural design of hard coatings //Progress in Materials Science. – 2006. – Vol. 51. – P. 1032-1114.
6. Musil J. Hard and superhard nanocomposite coatings//Surface and Coatings Technology. – 2000. – Vol. 125. – P. 322-330.

7. Andrievski R.A. Nanomaterials based on high-melting carbides, nitrides and borides//Russian Chemestri Reviews. – 2005. – Vol. 74. – P. 1061-1072.
8. Musil J. Hard nanocomposite coatings: Thermal stability, oxidation resistance and toughness// Surface and Coatings Technology. – 2012. – Vol. 207. – P. 50-65.
9. Pogrebnjak A.D., Ponomarev A.G., Shpak A.P., Kunitskii Yu.A. Application of micro- and nanoprobes to the analysis of small-sized 3D materials, nanosystems, and nanoobjects//Physics-Uspekhi. – 2012. – Vol. 55. – P. 270-300.
10. Pogrebnjak A., Danilionok M., Uglov V., Erdybaeva N., Kirik G., Dub S., Rusakov V., Shypylenko A., Zukovski P., Tuleushev Y. Nanocomposite Protective Coatings Based on Ti-N-Cr/Ni-Cr-B-Si-Fe, Their Structure and properties//Vacuum. – 2009. – Vol. 83. – P. 235-239.
11. Pogrebnjak A.D., Uglov V.V., Il'yashenko M.V., Beresnev V.M., Shpak A.P., Kaverin M.V., Erdybaeva N.K., Kunitskii Yu.A., Tyurin Yu.N., Kolisnichenko O.V., Makhmudov N.A., and Shypylenko A.P. Nano-Microcomposite and Combined Coatings on Ti-Si-NAA/C-Co-Cr/Steel and Ti-Si-N/$(Cr_3C_2)_{75}$-$(NiCr)_{25}$Base: Their Structure and Properties. Nanostructured Materials and Nanotechnology IV//Ceramic Engineering and Science Proceedings. – 2010. – Vol. 31. – P. 127-138.
12. Lavrent'ev V.I., Pogrebnyak A.D., Shandrik R. 'Evolyuciya vakansionnyh defektov v poverhnostnyh sloyah metalla pri impul'snom vozdejstvii 'elektronnym puchkom //Pis'ma v Zh'ETF. – 1997. – № 65. – P. 618-622.
13. Rempel'S.V., Gusev A.I. Poverhnostnaya segregaciya v raspadayuschihsya karbidnyh tverdyh rastvorah//Pis'ma v Zh'ETF. – 2008. – № 88. – P. 508-513.
14. Krause-Rehberg R., Leipner H.S. Positron Annihilation in Semiconductors: Defect Studies. – New York: Springer-Verlag Berlin Heidelberg, 2003. – 387 p.
15. Pogrebnjak A.D., Il'yashenko M.V., Kaverin M.V., Shypylenko A.P., Pshyk A.V., Beresnev V.M., Kirik G.V., Erdybayeva N.K., Makhmudov N.A., Kolisnichenko O.V., Tyurin Yu.N., Shpak A.P. Physical And Mechanical Properties of The Nanocomposite And Combined Ti-N-Si / WC-Co-Cr/ and Ti-N-Si/$(Cr_3C_2)_{75}$-$(NiCr)_{25}$ Coatings//Journal of Nano- and Electronic Physics. – 2009. – Vol. 1. – P. 66-77.
16. Pogrebnjak A.D., Mahmud A.M., Karasha I.T., Kirik G.V., Tkachenko R.Y., Shypylenko A.P. Structure and Physical-Mechanical Properties of nc-TiN Coatings Obtained by Vacuum-Arc Deposition and Deposition of HF Discharg//Journal of Nano- and Electronic Physics.– 2011.–Vol. 3. – P. 97-105.
17. Pogrebnjak A.D., Ruzimov Sh.M., Alontseva D.L., Zukowski P., Karwat C., Kozak C., Kolasik M. Structure and properties of coatings on Ni base deposited using a plasma jet before and after electron a beam irradiation//Vacuum. – 2007. – Vol. 81. – P. 1243.
18. Sobol' O.V., Pogrebnjak A.D., Beresnev V.M. Effect of the Preparation Conditions on Phase Composition, Structure, and Mechanical Characteristics of Vacuum-Arc Zr-Ti-Si-N Coatings// Phys. Met. Metallogr.– 2011.– Vol. 112. – P. 188.
19. Pogrebnjak A.D., Shpak A.P., Beresnev V.M., Kolesnikov D.A., Kunitskii Yu.A., Sobol O.V., Uglov V.V., Komarov F.F., Shypylenko A.P., Makhmudov N.A., Demyanenko A.A., Baidak V.S., and Grudnitskii V.V.. Effect of Thermal Annealing in Vacuum and in Air on Nanograin Sizes in Hard and Superhard Coatings Zr–Ti-Si-N//Journal of Nanoscience and Nanotechnology. – 2012. – Vol. 12.